A Study of Methanol Vapor Sorption Dynamics by Nafion Membranes

Ho Youn Ryu
April 14th, 2009
Advisor: Professor Jay B. Benziger, Professor Sankaran Sundaresan

Submitted in partial fulfillment
of the requirements for the degree of
Bachelor of Science in Engineering

Department of Chemical Engineering
and Material Science Certificate Program
Princeton University

This paper represents my own work in accordance with University regulations.

I authorize Princeton University to lend this thesis to other institutions or individuals for the purpose of scholarly research.

Ho Youn Ryu

I further authorize Princeton University to reproduce this thesis by photocopying or by other means, in total or in part, at the request of other institutions or individuals for the purpose of scholarly research.

Ho Youn Ryu

Princeton University requires the signatures of all persons using or photocopying this thesis. Please sign below, and give address and date.

To my family

Acknowledgements

I would like to first thank Professor Benziger for the giving me the opportunity to work on this exciting project. His guidance was vital to truly understanding the fundamentals of fuel cells and Nafion membranes.

I would also like to thank Professor Sundaresan for his support. It was difficult to find a senior thesis topic that really motivated me, but Professor Sundaresan, when I was on the other side of the globe, helped me find a topic that was exciting for me.

I also want to thank the graduate students in Professor Benziger's lab: Erin, Josh, and May Jean, who patiently helped me with everything from setup to understanding data. I could not have completed this project without their help.

I want to thank the people who morally supported me. Phone calls and video chats with my family in Korea helped me stay strong throughout the year. Although they were far away from Princeton, their moral support helped me focus during the tough times.

Abstract

Sorption dynamics of methanol by Nafion was studied in this thesis. Methanol's potential as a source of fuel in PEM fuel cells was the motivation behind this thesis. Methanol's molecular structure, coupled with Nafion's structure with hydrophilic and hydrophobic parts, led to much faster absorption than that of water. Methanol sorption data was measured at 30, 40, 50, and 60°C and used three different thicknesses of Nafion membranes: 50.4μm, 127μm, and 254μm. Results displayed a clear indication of departure from the Fickian diffusion model. Desorption was much faster than absorption, and both absorption and desorption collapsed to a universal curve when plotted against time/thickness, not time/thickness^2. Results were compared with results from various viscoelastic studies on Nafion and the reasons for the differences between methanol and water sorption were provided. Also, through analysis of data, kinetic parameters of methanol sorption and a model for methanol absorption were obtained.

Table of Contents

List of Figures

List of Tables

1.1 Fuel Cells: Overview

1.1.1 Why Fuel Cells?

The rapid depletion of petroleum sources and escalating global warming are two of the many motivations behind the enthusiastic search for renewable energy sources. Fuel cell technology is one promising alternative to petroleum-based technologies because fuel cells use hydrogen rather than hydrocarbons and thus emits no CO_2. Even if methanol were used as fuel, fuel cell vehicles would emit half the amount of CO_2 as today's gasoline combustion vehicles[1]. In addition to the environmental advantages, fuel cells also provide relatively high efficiency, because heat engine efficiency is thermodynamically limited by temperature whereas fuel cell efficiency is not[7].

1.1.2 Fuel Cells with Methanol as Fuel

Although hydrogen first comes to mind in the discussion of fuel cells, methanol is an alternative with its own advantages. There are several reasons for using methanol as fuel over directly utilizing hydrogen. First of all, it is liquid at room temperature and ambient pressure, while by comparison hydrogen gas needs to be stored at high pressure. Secondly, methanol contains no sulfur, which is known to contaminate fuel cells. The downside of using methanol as fuel is that obtaining hydrogen from methanol does require the use of a reformer. Reformers impose both space and weight restrictions to the device. Also, small amounts of emissions are detected in methanol fuel cells[1].

1.1.3 How a Fuel Cell Works

The overarching theory behind fuel cells is simple. The two oxidation-reduction reactions of reverse water electrolysis are the main mechanism for producing electric energy from chemical energy. Several designs of fuel cells exist today, with the polymer

electrolyte membrane fuel cell (PEMFC) studied in this thesis. A generic PEMFC includes three major parts: an anode, a cathode, and a membrane separating the two electrodes, as shown in Figure 1-1.

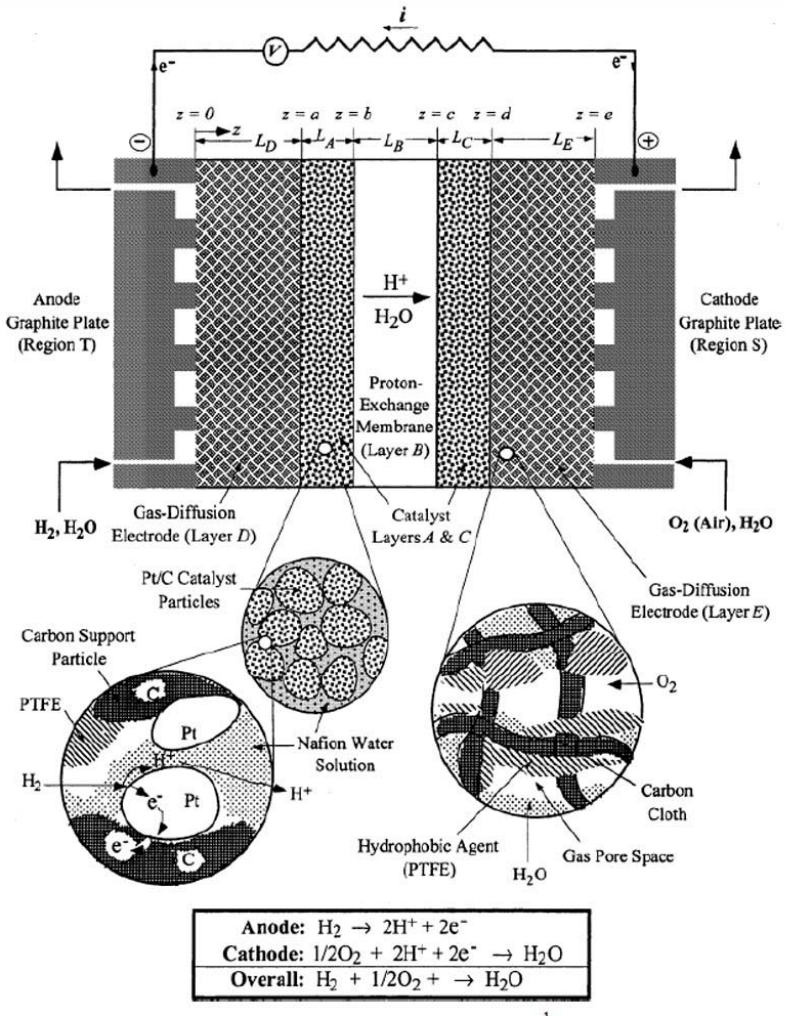

Figure 1-1 Diagram of PEMFC[28]

This assembly of anode-membrane-cathode is referred to as membrane electrode assembly (MEA). PEMFCs take H_2 at the anode and air at the cathode side. H_2 then diffuses through a gas diffusion layer (GDL) to reach the layer of catalysts. Here, hydrogen adsorbs onto Platinum catalysts and ionizes into two hydrogen ions and two electrons through the following oxidation reaction:

$$2H_2 \rightarrow 4H^+ + 4e^-$$

Once this oxidation reaction is completed, the product electrons travel through an external circuit to the cathode, providing current. At the same time, hydrogen ions move onto the third layer of polymer electrolyte membrane. This polymer electrolyte membrane is the distinguishing feature of PEMFC, and its performance is directly related to that of the fuel cell. Membranes are discussed in greater detail in the following section. While hydrogen ionizes into hydrogen ions and electrons at anode, the electrons that were stripped off from H_2 travel through an external circuit to the cathode. Oxygen is taken in at cathode and reacts with the excess electrons and the hydrogen ions to produce water through the following reactions:

$$O_2 + 4e^- + 4H^+ \rightarrow 2H_2O$$

The overall combination of these two half-reactions is that of electrolysis of water in reverse. The most important part of this process is proton conduction from the anode to the cathode as hydrogen ions from the anode become reactants at the cathode. Without hydrogen ion conduction, the overall reaction cannot be completed. Consequently, hydrogen ion conductivity is the most significant property of the polymer electrolyte membrane.

Despite the elegance of hydrogen fuel cell operation, storing hydrogen is difficult. This difficulty, however, can be eliminated by direct use of methanol as fuel. Besides easy storage, methanol offers other advantages, such as higher energy density, faster refill, and reduced weight of the system[19]. Fuel cell designs that directly use methanol as fuel are called direct methanol fuel cell (DMFC).

The designs of the PEM DMFCs resemble that of PEMFCs. What differentiates PEM DMFCs from PEMFCs is the oxidation reaction at anode. The overall reaction at anode becomes:

$$CH_3OH+H_2O \rightarrow 6H^+ + 6e^- + CO_2$$

Unfortunately, methanol has a carbon atom and ends up emitting CO_2. This CO_2 is purged at the anode. However, CO_2 emission from methanol fuel cells is significantly lower that the current level of emission in gasoline combustion engines[1].

It is clear from the diagram and the underlying chemistry behind fuel cells that these membranes must easily conduct hydrogen ion. These membranes must also separate the fuel from the oxidant and resist conducting electrons. The material that fulfills these requirements most satisfactorily is Nafion from DuPont[20], and Nafion is widely used in today's fuel cell designs.

1.2 Nafion

1.2.1 Nafion Overview

Nafion was first developed by DuPont Company in the late 1960's. It is a perfluorinated vinyl ether comonomer with tetrafluoroethylene (TFE). Its structure is shown in Figure 1-2 below.

Figure 1-2 Molecular Structure of Nafion[28]

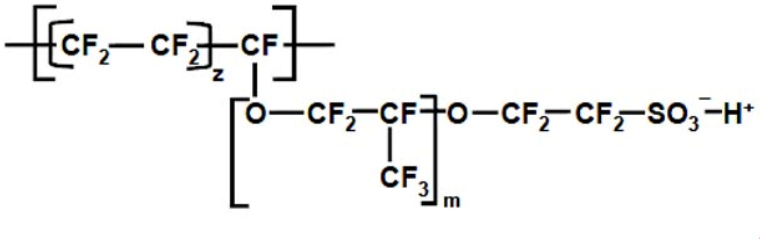

Nafion is considered the most suitable material for fuel cell designs because it fulfills the three aforementioned requirements for membranes. Although Nafion's properties are not ideal in each particular aspect, it possesses a good balance between proton conductivity, chemical stability, and mechanical toughness[28].

Equivalent weight (EW) represents the number of grams of Nafion per mole of sulfonic acid group. m in Figure 1-2 is related to EW by EW = 100m+446[21]. Nafion produced today has EW of 1100g/mol, and side chains are separated by 14 CF_2 units[20]. DuPont has its own convention of naming Nafion with various EW and thicknesses. In DuPont naming convention, EW is first stated, followed by thickness. For example, Nafion with EW of 1100g/mol and thickness of 0.005 inches would be named Nafion 115. Similarly, Nafion with EW=1100g/mol and thickness = 0.010 inches would be named Nafion 1110. Currently Nafion 112, 1135, 115, 117, and 1110 are commercially available[28].

Since the introduction of Nafion, the morphology thereof has been researched extensively. However, due to the indirect method involved in examining the structure of Nafion and the random chemical structure of Nafion that allowing it to freely form ionic and crystalline domains, the exact morphology of Nafion is yet to be completely understood[21]. Thus far, numerous technologies, ranging from small-angle X-ray scattering (SAXS) to tunneling electron microscope (TEM), have been the main method of looking at Nafion's structure. Mauritz and Morre[21], out of University of Southern Mississippi, reviewed Nafion morphology and, though their models used crude assumptions, their work still gives helpful insight in the understanding of Nafion.

Although current methods of inspecting Nafion morphology are somewhat imprecise, researchers conclude with certainty that Nafion phase separates into distinct hydrophobic and hydrophilic regions. The chemical representation of Nafion in Figure 1-2 depicts the two distinct portions of Nafion: hydrophobic TFE backbone region and hydrophilic region with SO_3^- end group. When humidity is introduced to Nafion, hydrophilic region will pick up humidity, swell and changes its structure to allow transport of the hydrogen ion[20].

Mauritz and Moore[21] discuss several plausible models for Nafion morphology and behavior in their paper. Of the discussed models, those of Gierke et al.[11] and Haubold et al.[12] most lucidly model the relationship between Nafion structure and the hydrogen transport phenomenon. These two models are discussed in the following paragraphs.

The model proposed by Gierke et al.[11] is the cornerstone of Nafion morphology research. Although the model of Gierke and co-workers[11] did not account for some of the properties such as crystallinity of the perfluorocarbon backbone, it provided the rationale behind ion and water transport of Nafion. And their model has been accepted as plausible for many years[20]. Gierke et al.'s[11] model is the cluster-network model. In the cluster-network model, clusters of sulfonate groups are arranged in a spherical pattern. Spherical clusters of sulfonate groups are connected by channels that allow for water/ion transport. An illustration of this cluster-network model, which has the shape of inverted micelles, is in Figure 1-3.

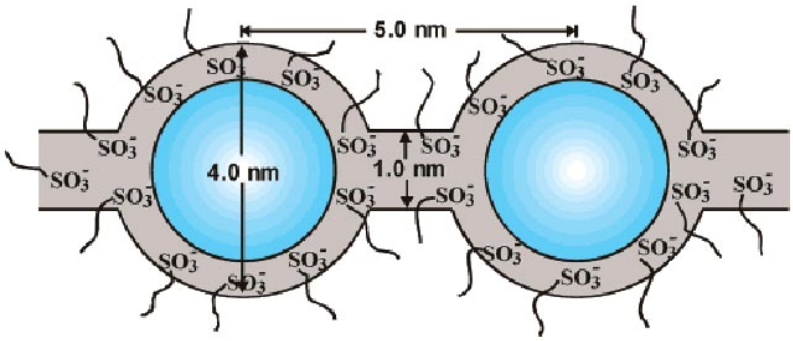

Figure 1-3 Diagram of the clustered model (inverted Micelles)[21]

More recent studies of Nafion morphology yielded improvements on Gierke et al.'s[11] cluster-network model. A sandwich-like model proposed by Haubold et al.[12] is one of these adaptations and is so-named because it supposes a core region is placed in between layers of shell regions. The shell region has the TFE backbone on the outermost part, and the chain with sulfonate end group hanging down from the backbone. The bottom shell region has the same structure except that the chain originates from below. Sulfonate groups of the top shell and the bottom shell come together in the middle, but are repelled by each other due to electrical charge. This repulsion creates a space, which is referred to as the core region. In the sandwich-like model, the core region explains the water/ion transport phenomenon by providing a channel for the transport to occur. This second model is of special relevance to this thesis because it was presented within the context of direct methanol fuel cell membranes[21]. Haubold et al.[12] concluded that methanol "leaves the side chains nearly unaffected." A diagram of the sandwich-like model is presented in Figure 1-4.

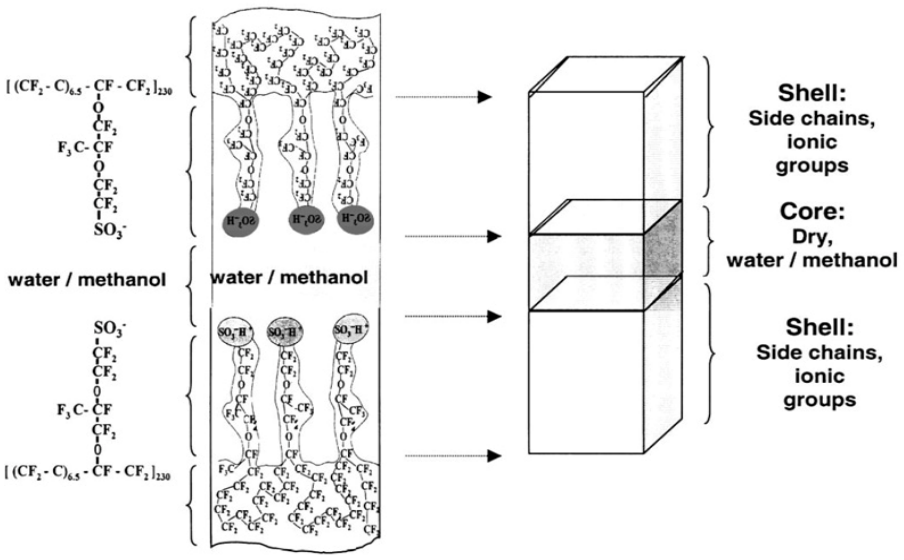

Figure 1-4 Diagram of the sandwich-like model of Nafion[21]

1.2.2 Water and Methanol Management

Water management and fuel cell performance are closely related, and controlling water flow in fuel cells for optimal performance poses a great challenge in engineering fuel cell designs. Generally, water content is directly proportional to proton conductivity. Yang et al.[31] plotted the relationship between the two quantities by measuring specific conductivity of Nafion against water activity (P_w/P_{sat}) in Figure 1-5.

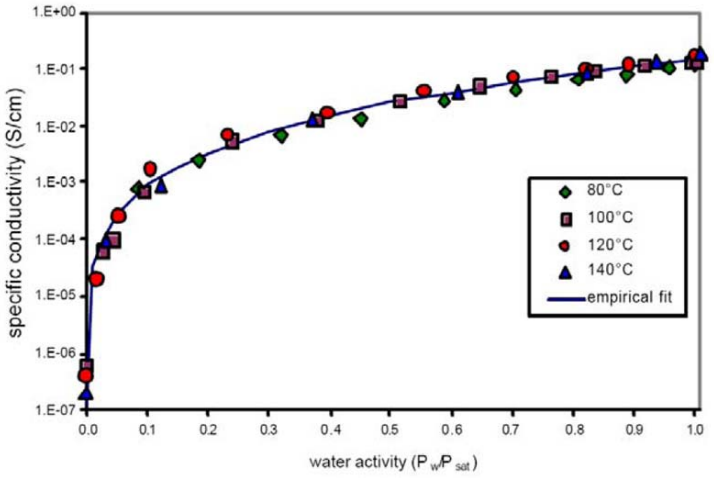

Figure 1-5 Proton conductivity of Nafion plotted against water activity[30]

Water content and proportion can also negatively affect fuel cell performance in various ways including through electro-osmotic drag, with the dry-out effects of air, and in the uneven distribution of water, etc[19]. Electro-osmotic drag occurs when hydrogen ions move from the anode to the cathode. When hydrogen ions travel, they tend to drag water molecules with them. This implies that the anode side can dry out and adversely affect fuel cell performance. Secondly, at high temperatures air dries out water. Larmine and Dicks[19], in their overview of fuel cells, state that "it suffices to say that at temperatures of over approximately 60°C, the air will always dry out the electrodes faster than the water is produced." Thirdly, the uneven distribution of water results in the hydration of some cells while others dry out. This happens if dry air enters and picks up water half way through, which ends up leaving the cell as humidified air[19]. Additionally, flooding electrodes and blocking pores to the electrodes or GDL can hinder fuel cell performance as well. Because of these difficulties, managing water in a fuel cell is a challenging task.

Like water, methanol needs to be managed in order to ensure optimal fuel cell performance. One of the problems associated with methanol management is fuel crossover[7, 13, 32]. Fuel crossover refers to transport of methanol from the anode to the cathode. Normally, methanol is expected to react with water to produce hydrogen ions at the anode. Unfortunately, methanol readily mixes with water and thus is able to reach the cathode. This fuel crossover results in waste of fuel and reduction in the cell voltage, which is referred as a mixed potential[19].

Fuel crossover can be quantified by measuring the current that would have been produced had the fuel not crossed over to the cathode, defined as a crossover current[19]. i_c,

crossover current, can be used alongside with *i,* useful output current of the fuel cell, to yield fuel utilization coefficient n_f.

$$n_f = \frac{i}{i + i_c} \quad \text{(Eq. 1)}$$

Though values as high as 0.85 to 0.90 have been reported for n_f, 0.80 is a typical value[18].

1.3 Non-Fickian Water Sorption Dynamics of Nafion Membranes

Water and methanol management are directly related to the overall efficiency of fuel cells. Dry membranes exhibit conductivities that are several orders of magnitude lower than those of saturated membranes[31], and methanol crossovers adversely affect overall output. Yang et al.'s[31] paper sheds light on the importance of hydration level optimization in fuel cell design. Yang and co-workers[31] measured Nafion conductivity against water activity, and demonstrated the relationship between them. These measurements show a five order of magnitude increase in conductivity with a water activity increase from 0 to 1. The data are plotted in Figure 1-5

Methanol management is very important. Because of methanol's high permeability through Nafion, the performances of DMFCs are limited by mixed potential caused by methanol crossover. To remedy this problem, low concentrations of methanol are used. When methanol concentration is too high, the cell voltage drops significantly and oxygen loss occurs at cathode[28]. Scott et al.[29] demonstrated this relationship by plotting open circuit voltage against methanol concentration. Figure 1-6 shows the plot.

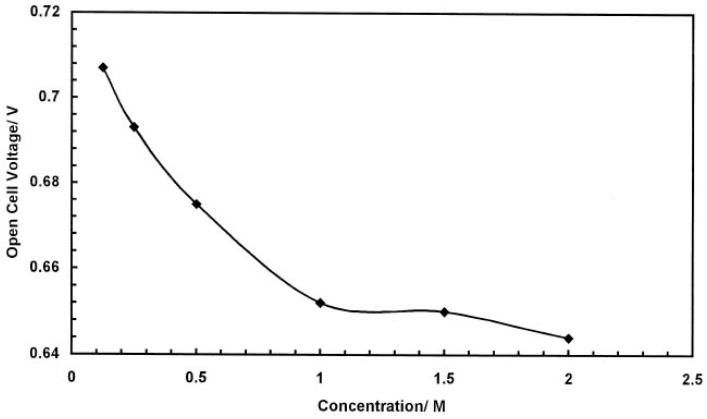

Figure 1-6 Open cell voltage of fuel cell(V) plotted against methanol concentration(M)[29]

The close relationship between conductivity and water and methanol management underscores the importance of careful studies on water and methanol sorption dynamics by Nafion. Studies on water sorption dynamics by Nafion have been conducted by Satterfield[28] at Princeton University as her Ph.D. thesis under the guidance of Professor Benizger.

Many researchers[2, 9, 22, 26, 30, 33] have completed studies on water sorption and transport in Nafion before Satterfield. In her dissertation, Satterfield[26] cites eleven authors, who focused on studying diffusion coefficients and/or other mass-transfer kinetics via dynamic water uptake and/or loss, steady-state permeation, and NMR diffusion measurements. The models proposed by these researchers assumed Fickian diffusion equations, (Eq. 2).

$$\frac{\partial C}{\partial t} = D\frac{\partial^2 C}{\partial x^2} \quad \text{(Eq. 2)}$$

Yet clear deviations from Fickian diffusive behavior have been detected. In Fickian diffusion models, diffusion coefficients do not depend on concentrations, do not discriminate between liquid and vapor, and do not have dissimilar behaviors for

absorption and desorption. Researchers[3-5] in the past have noticed these deviations and attributed them to several factors, such as water activity gradient, localized temperature effects, interfacial mass transport, and structural changes[2, 9, 22, 26, 30].

What distinguishes Satterfield's[28] research from others is that she proposed interfacial mass transport and polymer relaxation dynamics as the rationale behind non-Fickian sorption dynamics by Nafion. To reach this conclusion, Satterfield[28] used a self-devised sorption dynamics experimental setup. She collected sorption and desorption data, which clearly exhibited non-Fickian sorption dynamics of Nafion membranes. Satterfield[28] demonstrated this by plotting an approach to final mass change, which is $(M_t-M_o)/(M_\infty-M_o)$ for absorption and $(M_o-M_t)/(M_o-M_\infty)$ for desorption. These quantities were plotted against time. The most obvious deviation from Fickian diffusion is the dissimilar behaviors in absorption and desorption processes. Figure 1-7 shows this difference. The absorption curve takes around 5000 seconds to equilibrate while desorption proceeds much faster, taking only around 600 seconds to equilibrate. The sorption kinetics also varied with varying membrane thicknesses, as shown in Figure 1-7.

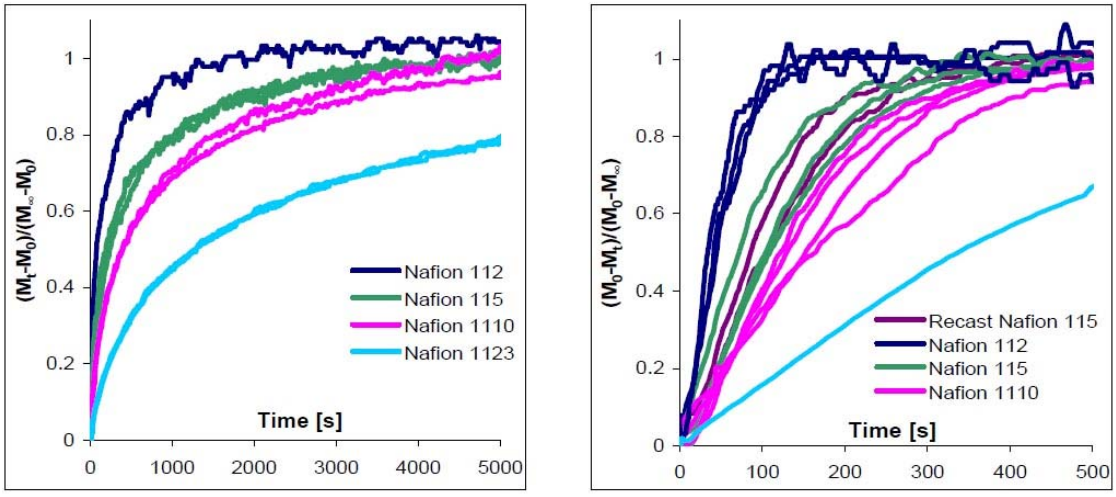

Figure 1- 7 Comparison of absorption and desorption kinetics by Nafion at 50°C at indicated membrane thicknesses[28]

Additionally, the curves collapsed to one curve when plotted against t/*l* but did not do so when plotted against t/l^2 (t: time, *l:* membrane thickness). This marks a departure from Fickian diffusive model because the solution to the Fickian model (Eq. 3) indicates that curves should collapse on to a universal curve when plotted against t/l^2.

$$\frac{M_t - M_0}{M_\infty - M_0} = 1 - \frac{8}{\pi^2}\sum_{m=0}^{m=\infty}\frac{1}{(2m+1)^2}\exp\left\{\frac{-D(2m+1)^2\pi^2}{4\ell^2}t\right\}$$

(Eq. 3)[28]

Satterfield[28] reported increase speed for both absorption and desorption curves with increasing temperature.

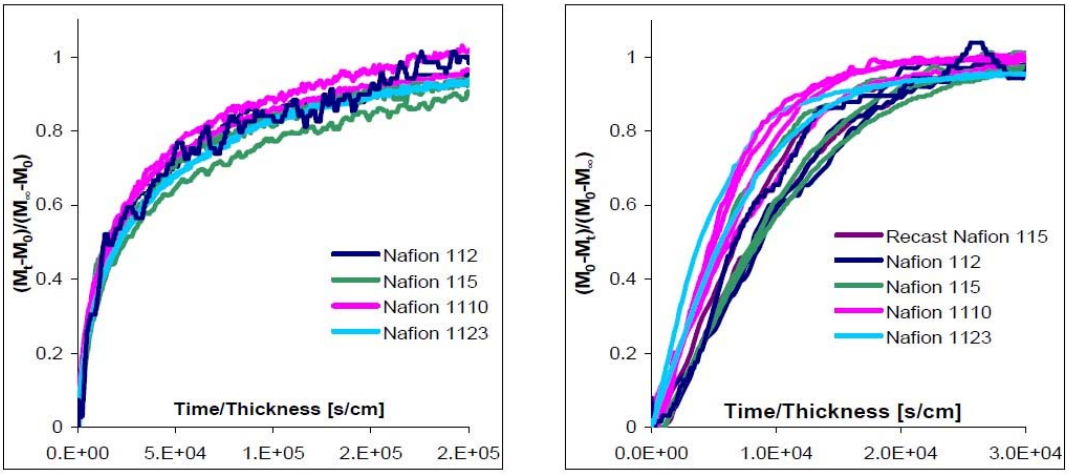

Figure 1-8 Comparison of absorption and desorption plotted against time/thickness by Nafion at 50°C at indicated membrane thicknesses[28]

Satterfield[28] states in her dissertation that deviations from the Fickian model in Nafion membranes are not due to structural changes because of the definitions of thickness and length are such that they contain a certain mass of polymer per unit area[28]. In other words, a given reference frame contains the same proportional mass of polymer at all time. The deviations from the Fick's model can be attributed to various physical deviations the assumptions in the Fick's idealized case. For example, Fick's model assumes that the diffusion coefficient D is not dependent on the concentration of the penetrant. In other words, a diffusion coefficient that does depend on concentration could explain the mechanism behind this non-Fickian behavior. Satterfield[28] proposed two-stage absorption as the mechanism behind the non-Fickian behavior by Nafion membranes, however. In two-stage absorption, there is an initial step where the polymer uptakes penetrant to a quasi-equilibrium value. This step is diffusion-controlled. After the initial step, polymer chains reconfigure themselves to allow for greater uptake of the solvent. This step is controlled by stress-relaxation characteristics of the polymer.

Based on her findings, Satterfield[28] found a model for absorption, (Eq. 4).

$$\frac{M_t - M_0}{M_\infty - M_0} = \varphi\left\{1 - \exp\left[-\frac{k_{\text{int}} t}{\ell}\right]\right\} + (1-\varphi)\{1 - \exp[-\beta t]\}$$

(Eq. 4)[28]

This model depends on three parameters: the interfacial mass transfer coefficient, k_{int}, the relaxation rate β ,and the weighting factor φ. The value for φ was 0.35 while values for β ranged from $5x10^3$ s^{-1} to $2x10^4$ s^{-1}. Values for k_{int} are summarized in Table 1 below.

Membrane Name, Thickness[μm]	k_{int} [cm/s]	E_A [kJ/mol]
112, 50.8	0.35	22.2
115, 127	10.2	30.6
1110, 254	10.6	29.8
1123, 606	7.6	28.8

Table 1-1 Reported values of interfacial mass transport coefficients and activation energy for various membrane thicknesses[28].

The model and actual data are plotted on the same domain in Figure 1-9.

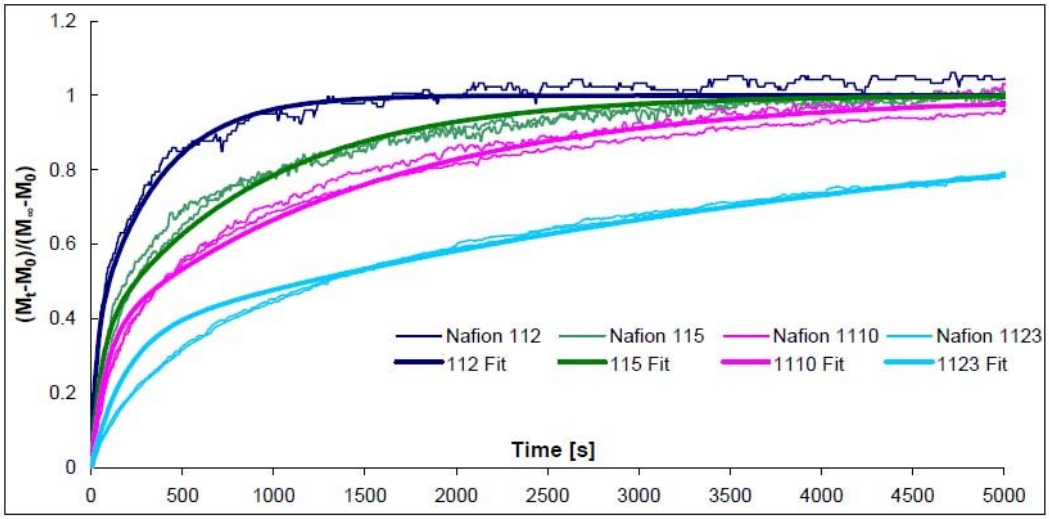

Figure 1-9. Model of water absorption proposed by Satterfield[28].

1.4 Thesis Objective

Satterfield's[28] findings on water sorption dynamics by Nafion membranes provided tremendous insight for fuel cell research. As interest in DMFC for use in the transportation sector rises, the importance of understanding methanol sorption dynamics in Nafion also increases. This thesis aims to comprehend the methanol sorption dynamics by Nafion membranes and compare the results with that of water sorption dynamics to obtain further understanding of Nafion's properties and structure.

2. Experimental Setup and Procedure

Procedure for this thesis was mainly adopted from Satterfield's study of water sorption dynamics by Nafion. To study methanol sorption dynamics, Nafion membranes with thicknesses of 50.8μm, 127μm, and 254μm were used. These DuPont products were obtained from Ion Power (New Castle, Del). Before using them in experiments, they were treated in four steps for clean-up. First, the membranes were boiled in 3% hydrogen peroxide for 1 hour, followed by 1 hour of boiling in de-ionized water. Then they were boiled in 1M sulfuric acid for 1 hour. And they were boiled again in de-ionized water for 1 hour. Once these membranes were cleaned, they were stored in liquid water at room temperature. Immediately prior to each trial, all of the membranes were dried to remove any water from the membrane. They were dried at 70°C for 2 hours over drierite.

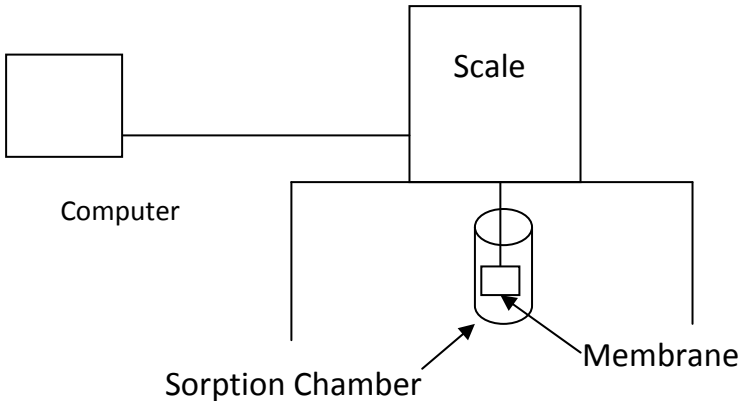

Figure 2-1 Schematic of the experimental setup

Figure 2-1 is a schematic of the experimental setup used. From the bottom of the scale hangs a string. The bottom end of the string is shaped like a hook, and each membrane was hung on this hook in each trial. The setup in whole is photographed in Figure 2-2. Once the membrane and string were in place, these two parts were placed inside the sorption chamber. The right side of Figure 2-2 is the picture of the sorption chamber. Sorption chamber wrapped around with heating tape to control the temperature inside the chamber. The chamber was filled with methanol and was assumed to maintain methanol vapors saturated. Once the membrane was placed in the chamber, the scale started measuring the weight of the membranes. The lid to the chamber was kept 2°C above the set temperature in order to prevent condensation on the wire. Used membranes were placed in a closed container with methanol inside. The overnight mass uptake from the container was less than 5% for each trial, which indicates that methanol vapors were indeed saturated inside the chamber.

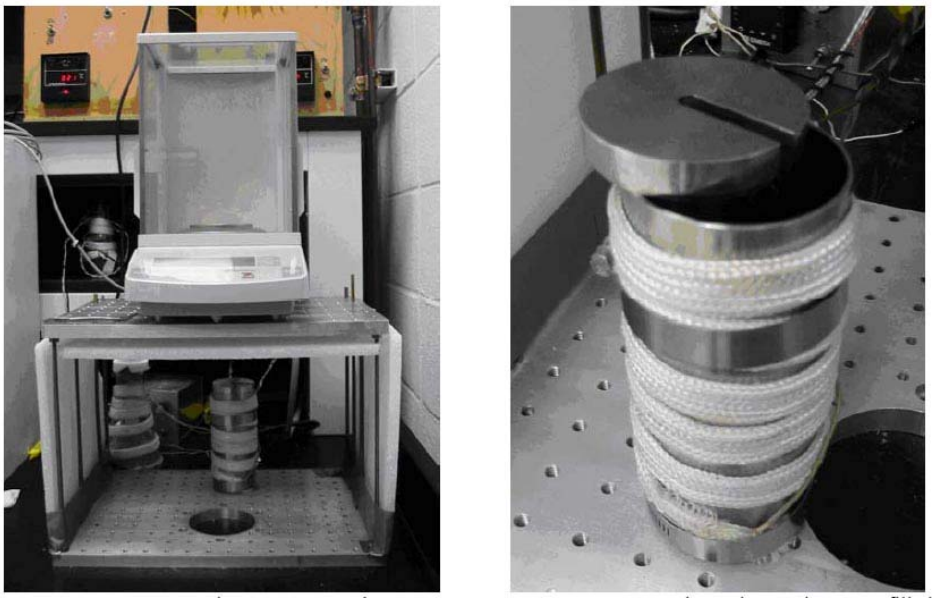

Figure 2-2 Photograph of the experimental setup (left) and a close-up photograph of the sorption chamber (right), photograph adopted from [28]

For desorption experiments, membranes were exposed to the saturated methanol vapor for 1 hour, which, based on the absorption experiments, was sufficiently long to fully saturate the membranes. A photograph of this membrane-saturation setup is shown in Figure 2-3. Afterwards, membranes were placed inside the sorption chamber without methanol and the change in weight was measured using the scale. Instead of methanol, the chamber had zeolite to adsorb methanol and create a vapor activity of ~0.

Figure 2-3 Photograph of the saturation station. Membranes were exposed to 100% relative humidity condition in this saturation process.

The chamber is made out of stainless steel, and is 15cm tall and 6 cm in diameter. The lid was also stainless steel, and is 13mm in thickness. The scale used in this experiment was an Ohaus AR0640, accurate to 10^{-4}g. The scale is connected to a computer, which used LabTech software to collect data every 2 seconds.

3. Results

The difference between absorption and desorption kinetics is one of the qualities that indicates a departure from the Fickian model. In Figure 3-1, absorption data are plotted while, in Figure 3-2, desorption data are plotted. Each line in both figures indicates one experiment carried out at 50°C for the indicated membrane thickness.

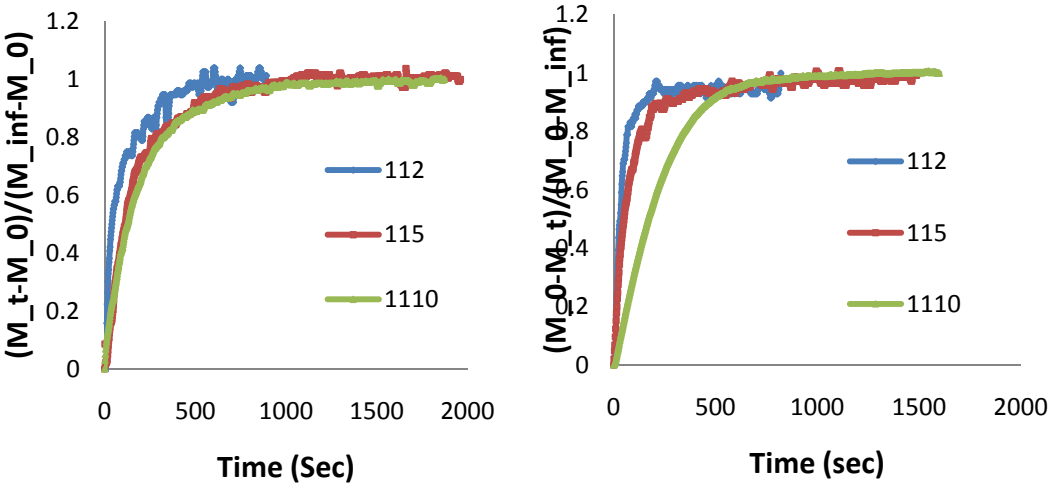

Figure 3-1(left), 3-2(right). Plot of mass uptake of methanol against time (3-1) and mass loss of methanol against time (3-2)

For absorption, methanol mass uptake, $(M_t-M_0)/(M_\infty-M_0)$, is plotted against time while mass loss, $(M_0-M_t)/(M_0-M_\infty)$, is plotted for desorption. In these plots, desorption is faster than absorption for each thickness. For all thicknesses, absorption curves equilibrate around 1100 seconds. In desorption, for all thicknesses it took approximately 600 seconds which is close to ½ of the time it took for absorption.

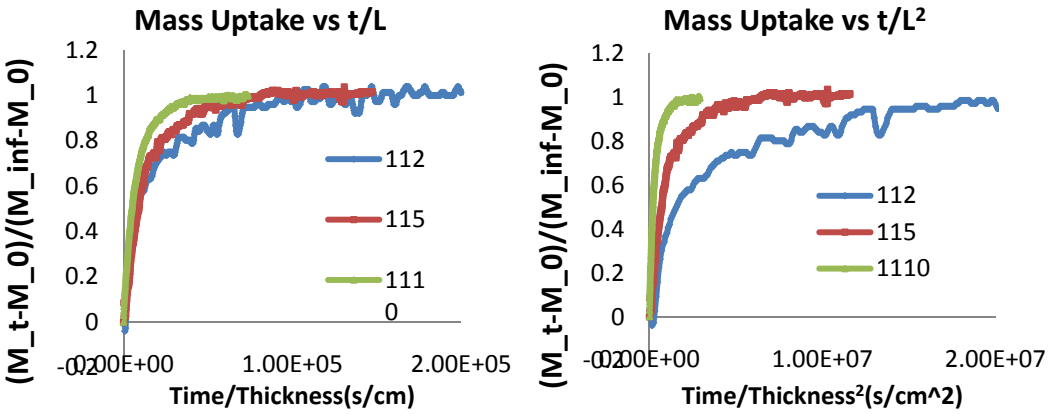

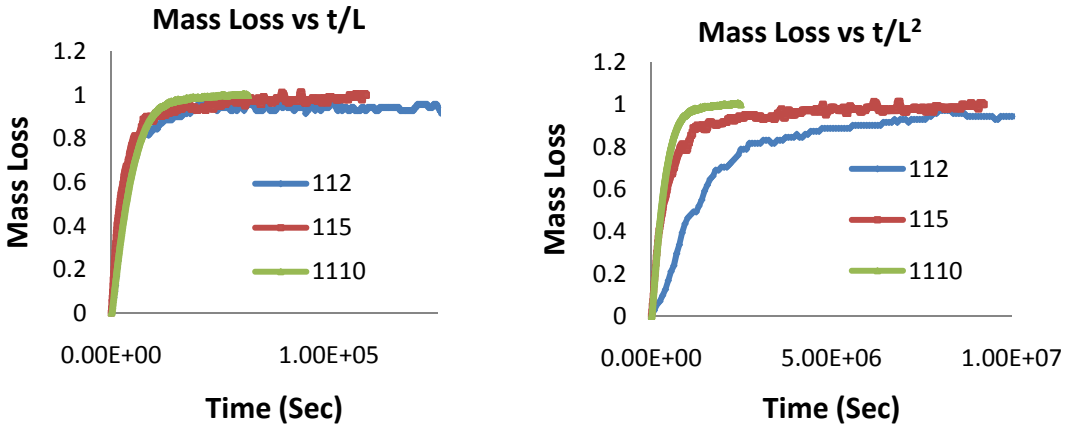

Figure 3-3(Top-left), 4(Bottom-left), 5(Top –right), 6(Bottom-right) Absorption curves are plotted against time/thickness(3-3) and time/thickness^2(3-5). On the bottom, desorption curves are plotted against time/thickness (3-4) and time/thickness^2(3-6)

Figure 3-3 through 3-6 also exhibit a departure from the Fickian model. Plotting the absorption and desorption data against t/l (t: time, l: membrane thickness) and t/l^2 is a good way to demonstrate whether or not the behaviors of the curves are Fickian. Figure 3-3 and 3-4 show absorption data plotted against t/l and t/l^2 while Figure 3-5 and 3-6 show desorption data plotted against t/l and t/l^2 at 50°C. Both absorption and desorption data collapse onto a universal curve when plotted against t/l but diverge when plotted against t/l^2. Had Fickian diffusion controlled the sorption dynamics, the opposite would have been true; sorption curves would have collapsed onto one curve when plotted against t/l^2.

Another independent variable that was adjusted for each run was the ambient temperature. Experiments were conducted at four different temperatures: 30, 40, 50 and 60°C. As temperature is raised, both absorption and desorption kinetics increased speed. Although kinetics at 40°C and 50°C are similar to each other, there is a pronounced increase in sorption speed when the temperature is increased from 30°C to 60°C. Figure

3-7 show plots of Nafion 115 sorption dynamics at varying temperatures, which show the increasing trend with temperature.

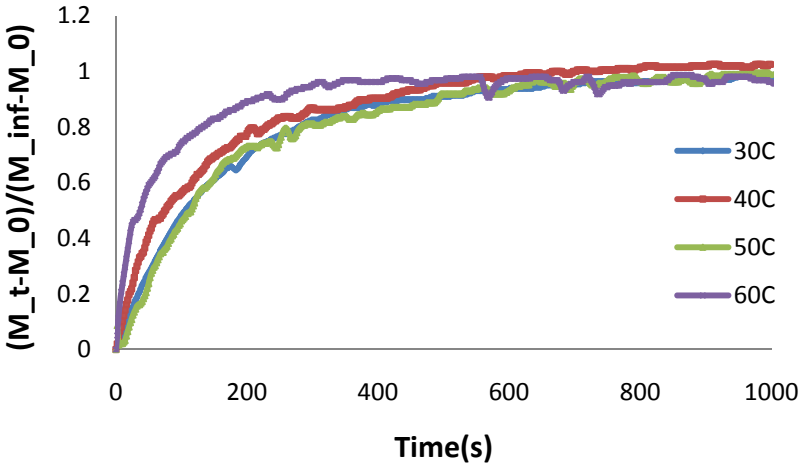

Figure 3-7 Absorption curves are plotted against time at varying temperatures (30°C-60°C). Membrane thickness 0.005" (Nafion 115)

The trends of sorption dynamics mentioned in this section are true for all experiments, and the curve presented above is a representative one with membrane thickness 0.005 inches. The results show that methanol sorption dynamics resemble those of water sorption. Also, desorption proceeds faster than absorption, increased temperature and membrane thickness both couple with faster kinetics. Insights gained from these comparisons are analyzed in the Discussion section of this thesis.

4. Discussion

The results from the experiments lead us to several questions that get to the fundamentals of methanol sorption phenomena. What is the right way to describe methanol sorption and desorption in Nafion and what are the mechanisms behind the

phenomena? In this regard, comparing methanol sorption to water sorption yields useful information. In this section, methanol sorption is first compared to water sorption. The diverging behavior of methanol and water sheds light on Nafion membranes' differing interactions with the two solvents. The dissimilarities between methanol and water sorption dynamics are examined with results from other experiments. Next, desorption of methanol is analyzed to establish various kinetic parameters, and finally, a new model for the sorption dynamics of the Nafion/methanol system is proposed. Methods of analyzing sorption data were adopted from Satterfield[28].

4.1 Comparison between Methanol and Water

The most striking outcome from methanol sorption experiments is that methanol absorption is much faster than water absorption, while desorption kinetics for both methanol and water are similar. Water absorption curves equilibrated at around 5000 seconds while methanol took only approximately 600 seconds. Absorption kinetics of methanol and water by Nafion are qualitatively compared by comparing the time necessary for mass uptake to reach equilibrium. Equilibrium times for water and methanol are plotted against temperature in Figure 4-1 and 4-2 below.

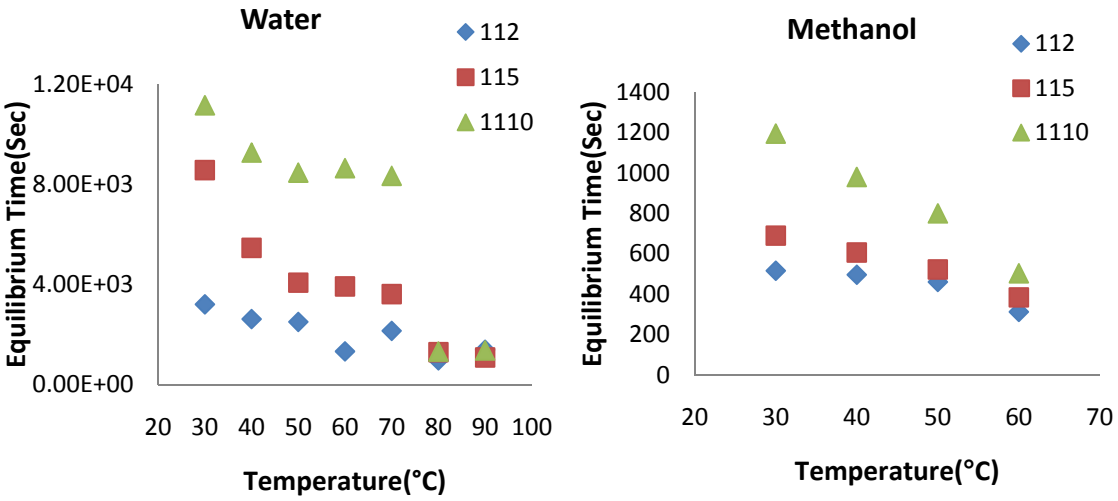

Figure 4-1 (left), 4-2(right) Time for water absorption to reach equilibrium plotted against temperature (4-1) and that for methanol (4-2). Errors are within the size of each point.

Three general terms are observed from Figures 4-1 and 4-2. First of all, thicker membranes take longer time to reach equilibrium. Nafion 1110 is the slowest to reach equilibrium at all temperatures and for both solvents in all cases. The reason for this trend is straightforward. Thicker membranes have more volume for mass uptake, and it takes longer to reach equilibrium. Secondly, membranes require less time to reach equilibrium as temperature increases. This trend can be contributed to increasing vapor pressure with increasing temperature. Lastly, methanol uptake is much faster than that of water even though their equilibrium time plots trend similarly. This trend takes more careful analysis to understand and is discussed in detail in the following sections.

4.1.1 Relationship between Sorption Kinetics and Vapor Pressure

Since the third trend shows that different solvents have differing sorption dynamics, it is important to first examine the differences between properties of the two solvents, especially between their boiling points and structures. Boiling points (BP) of

water and methanol differ by 35.3°C, (BP of water: 100°C, BP of methanol 64.7°C). Consequently, for a given temperature, methanol's vapor pressure is much higher than that of water. Table 4-1 lists vapor pressures of methanol and water at different temperatures.

Temp. (°C)	Vapor Pressure, Methanol (mmHg)	Vapor Pressure, Water (mmHg)
30	163.97	31.8
40	265.75	55.3
50	416.58	92.5
60	633.72	149.4
70	938.26	233.7
80	1355.47	355.1
90	1914.96	525.8

Table 4-1 List of vapor pressure for methanol and water for different temperatures

Vapor pressure of the solvent corresponds to the collision rate of gas molecules with the surface. If sorption dynamics are controlled by vapor pressure, not activity, then methanol sorption and water sorption of the membranes with equal thickness and vapor pressure would proceed similarly.

To investigate whether vapor pressures are closely related to the sorption dynamics of methanol and water, sorption dynamics of the two solvents with 1110 are compared at the same vapor pressure. At 40°C, methanol takes 981 seconds to equilibrate and has a vapor pressure of 265.75 mmHg. Water has the same vapor pressure at 73°C and if the sorption dynamics were controlled by vapor pressure, water sorption at 73°C should yield the same type of behavior as that of methanol at 40°C. As we only have data for water at 70°C and 80°C, a linear fit was taken between 70°C and 80°C to estimate how long it would have taken for water sorption to equilibrate at 73°C. Since sorption takes 8340 seconds at 70°C and 1326 seconds ay 80°C, the linear fit from these two

points yield 5798 seconds at 73°C. Another comparison was made at the same vapor pressures but at different membrane thickness, using Nafion 115. At 70°C sorption took 3621 seconds while only taking 1302 seconds at 80°C. Again, from a linear fit, an expected equilibration time at 73°C is calculated, which is 2925 seconds. Nevertheless, sorption at 40°C took 521 seconds with methanol. This is only 18% what is expected from water vapor pressure data, and the absorption kinetics at this thickness seems to be controlled by factors other than vapor pressure. Finally with Nafion 112, at 70°C, water sorption took over 2152 seconds while only taking around 973 seconds at 80°C. At same thickness and 40°C methanol also took around 500 seconds to equilibrate.

As methanol and water absorption kinetics at equal vapor pressure do not correspond to each other, vapor pressure is not the rate controlling mechanism behind sorption dynamics by Nafion membranes. Since boiling point difference did not yield a plausible rationale, structural differences are examined next.

4.1.2 Structural Difference between Water and Methanol

Equilibrium time plots of methanol and water indicated that methanol absorption is faster than that of water by an order of magnitude, and, in this section, the difference between methanol and water sorption dynamics is explained by looking at structural differences between the two. Before looking at structural differences between the two solvents, however, we must look at plots of $ln\left[\frac{M_0-M_t}{M_0-M_\infty}\right]$ of methanol and water at varying time/thickness. In these plots, distinct dissimilarities between methanol and water behaviors are observed. Figures 4-3 and 4-4 show $ln\left[\frac{M_0-M_t}{M_0-M_\infty}\right]$ plot for the both solvents at 50°C.

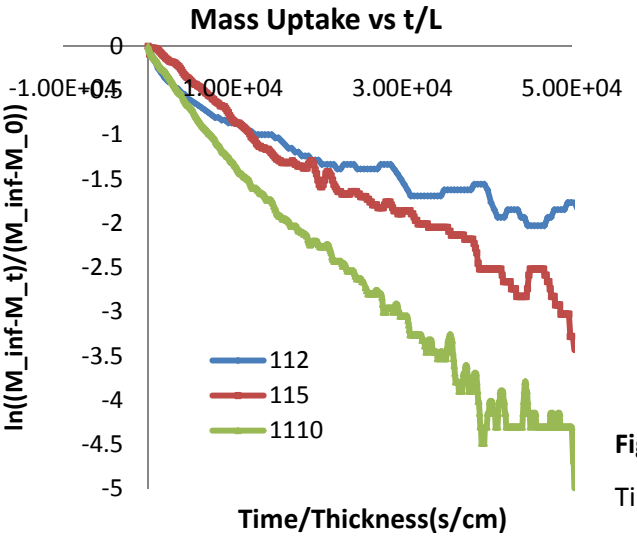

Figure 4-3 $ln\left[\frac{M_0-M_t}{M_0-M_\infty}\right]$ plotted against Time/Thickness, Methanol at 50°C

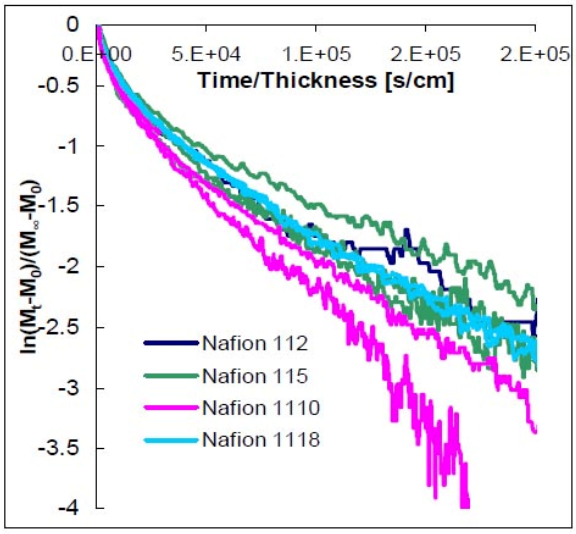

Figure 4-4 $ln\left[\frac{M_0-M_t}{M_0-M_\infty}\right]$ plotted against Time/Thickness, Water at 50°C[28]

In Figure 4-4, the absorption curve of water has two parts. The first part shows a fast early response to mass uptake, with a subsequent transition into a slower and linear second part. If absorption of water by Nafion were controlled by a single factor, namely either diffusion or interfacial mass transport, the curve would not split into two parts as shown. It would have a uniform rate of uptake throughout the process. For this reason, Satterfield[28] concluded that there is a transition between the two different rate-controlling mechanisms for water absorption.

Satterfield[28] also proposed that after an initial mass uptake by Nafion, the rate of polymer relaxation controls the kinetics of water absorption. In Satterfield's proposal, she used Gierke et al.'s[11] cluster model to explain her rationale. As shown in Figure 1-3, the fluorocarbon backbone surrounds the area where water is taken in. As Nafion picks up water the backbone stretches, thus increasing its volume for additional mass uptake. Satterfield[28] proposes that the rate of this swelling behavior is what governs the second portion of the absorption curve. The rates of stress relaxation phenomena by Nafion is extensively studied and presented by Satterfield in her dissertation[28].

In the methanol sorption plot in Figure 4-3, unlike water absorption curve in Figure 4-4, the slower second portion of the curve with fast response does not exist. Instead, throughout the absorption process, the curve linearly decreases with one rate constant. This means that methanol sorption kinetics is controlled by one mechanism throughout the entire mass uptake process. This single absorption rate can be explained by methanol's interaction with Nafion membranes.

As discussed in the introduction, Nafion's physical and chemical properties stem from its unique arrangement of hydrophobic TFE regions and hydrophilic chains with sulfonic end groups. These two regions interact differently with water and methanol, and this difference gives rise to diverging responses to the two solvents. While TFE backbone of Nafion has negligible interaction with water and polymer chains must relax and stretch to allow for additional uptake of water after an initial uptake, the TFE region of Nafion readily interacts with methanol. As shown in Figure 4-5, the methyl group of methanol can show van der Waal's type of interaction with the TFE.

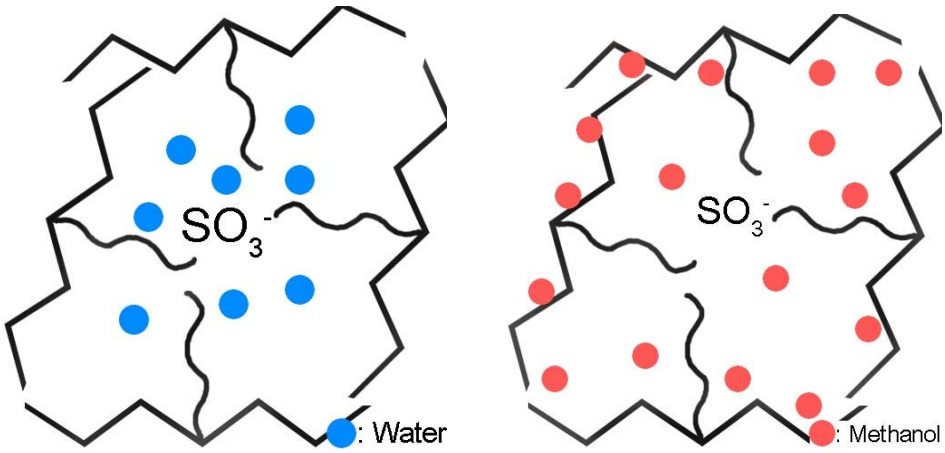

Figure 4-5 Depiction of water-Nafion interaction and methanol-Nafion interaction. Methanol's interaction with the TFE backbone allows greater volume for mass uptake

This interaction provides Nafion greater volume for methanol uptake. The hydrophobic region where water cannot penetrate is open to methanol, and because of this greater volume for mass uptake coupled with less resistance, methanol absorption is faster than that of water by an order of a magnitude.

Goswami et al.'s[10] study on wetting phenomena of Nafion by various solvents enumerates the differing mass uptake behaviors between the methanol and water. In their study, Goswami et al.[10] used Wilhelmy method to measure contact angles of water, methanol, and octane on several surfaces including Nafion and Teflon. The contact angles reported by Goswami et al. are listed below in Table 4-2 below:

Liquid/Substrate	Advancing Contact Angle	Receding Contact Angle	Sessile Drop Contact Angle
Water/Teflon	110	95	110
Water/Nafion	105	25	105
Water/Nafion on Carbon	110	40	110
Water/Nafion on Alumina	107	30	105
Octane/Teflon	20	15	>15
Octane/Nafion	n/a	n/a	>15
Methanol/Teflon	n/a	n/a	20
Methanol/Nafion	n/a	n/a	20

Table 4-2 List of contact angles of water, octane, and methanol on Nafion and Teflon surfaces[10]

As shown, advancing contact angles show that water poorly wets Nafion and Teflon, while methanol wets each surface well. Water's receding contact angle on Nafion, however, is 25°, which is a clear indication of successful wetting of Nafion's surface by water. This transition from poorly wetting to good wetting suggests that the surface morphology of Nafion undergoes a change from a hydrophobic state to a hydrophilic state[10]. In other words, water's contact with Nafion attracts hydrophilic sulfonic groups and repels hydrophobic TFE backbones. The additional time needed for this reconfiguration of Nafion means that water absorption takes more time than methanol absorption.

4.1.3 Transition of Nafion Morphology

What stands out from the plot of water equilibrium time versus temperature is the transitional region around 70°C. Between 30°C and 70°C, absorption kinetics' of different membrane thicknesses are distinctly dissimilar. At 30°C, the equilibrium time of Nafion 112 (thinnest membrane) and 115 differ by a factor of 10, and the difference between the longest and the shortest equilibrium time is around 7900 seconds. This value drops down

to 352 seconds at 80°C and further reduces to 277 seconds at 90°C. 277 seconds is only 3.5% of 7900 seconds. Reduction in equilibrium time across different membrane thicknesses eventually results in the collapse of equilibrium time values to a universal value around 80°C. At 80°C equilibrium times values of different thicknesses are within 25% of the median.

The methanol equilibrium time plot shows a similar trend. Values at lower temperatures are largely divergent but they get close to each other at higher temperatures. At 30°C the equilibrium time of Nafion 112 differs from that of Nafion 1110 by 680 seconds. This difference drops down to 190 seconds at 60°C. At 60°C, values are within 19% of the median value.

These transitional regions in both water and methanol absorption curves indicate a significant change in Nafion's properties and reasons behind the phenomenon need to be provided. In fact, similar phenomena have been observed by Majsztrik[20] and Ranney[25] at Princeton University, and their results will be compared with methanol and water sorption dynamics to yield further understanding of the Nafion membrane.

Under ambient conditions, Gierke et al.'s[11] cluster model (Figure 1-3) of Nafion provides a good picture of Nafion's molecular structure. The TFE backbone is placed on the outskirts of the cluster and sulfonic groups interact with each other via hydrogen bonding inside the cluster, and it forms a hydrophilic center. Nafion has a relatively high elastic modulus when the polymer chains are arranged with hydrophilic clustering in the center. Many investigators[6, 8, 14, 15, 16, 17, 18, 21, 23, 33], however, report a large decrease in elastic modulus at temperature near 80-90°C. Eisenberg[8] explains this significant decrease in elastic modulus by bringing attention to the balance between electrostatic

energy and elastic energy. At around room temperature, Nafion's energy state is lowered by clustering sulfonic groups together because electrostatic interactions between sulfonic groups can stabilize the molecule. Nevertheless, at a critical temperature T_c, Nafion molecules transition to a lower energy state by increasing their entropy. This means that clusters of sulfonic groups are broken and polymer chains increase its entropy by randomly orienting themselves. This loss of hydrophilic center results in the significant decrease in the elastic modulus of Nafion at T_c. In Figure 4-6, Eisenberg's[8] explanation, presented above, is depicted schematically.

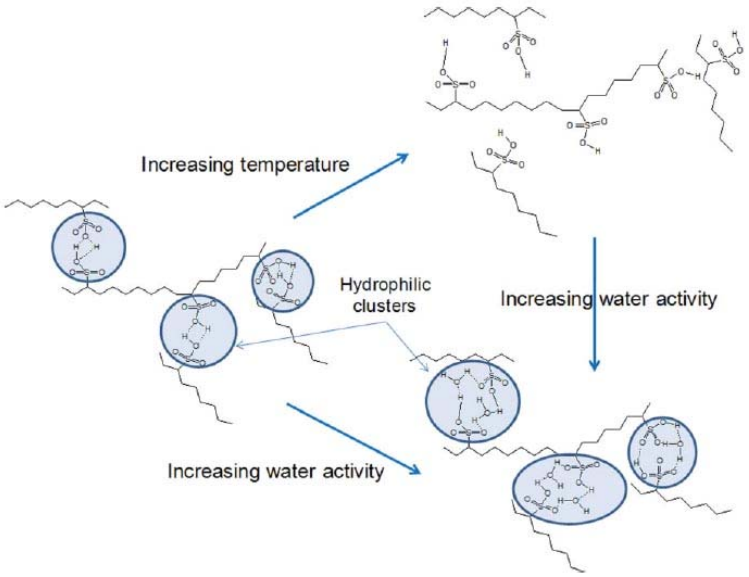

Figure 4-6 Nafion's transition from a clustered configuration to an entropy-driven state at a raised temperature.[27]

In Majsztrik's[20] study of the viscoelastic response of Nafion, Majsztrik[20] found a similar transitional temperature range for Nafion. Majsztrik's[20] experiments include a part in which he conducted experiments to find strain on Nafion at varying temperatures at zero water activity. His findings from this portion of the experiments are plotted in Figure 4-7.

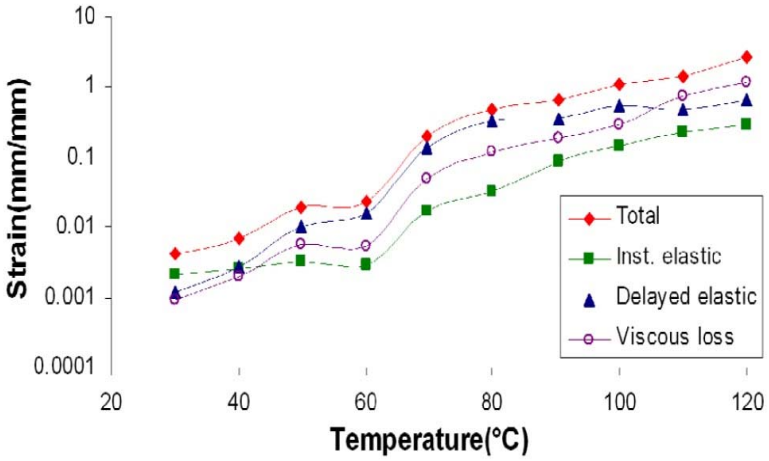

Figure 4-7 Strain vs Temperature plot, reported by [20]. Plot shows a transition region around 60°C

From this plot, the transitional period is observed. Around 60°C, the strain value undergoes a rapid increase showing a definite phase transition. As elastic modulus is defined:

$$\lambda = \frac{\sigma}{\epsilon}, \lambda\text{: elastic modulus, } \sigma\text{: Stress, } \varepsilon\text{: Strain} \qquad \text{(Eq. 5)}$$

the increase in strain, measured by Majsztrik[20], agrees well with Satterfield's[27, 28] findings on decrease in elastic modulus and Eisenberg's[8] rationalization on transition between hydrophilic clustering to random orientation of the polymer chains at elevated temperatures. Although water absorption data indicates that the transition starts to occur around 70°C, that of methanol starts occurring around 60°C (from the equilibrium time versus temperature plot, presented in Figure 4-2), which indicates that the critical temperature for transition has a value between 60°C and 70°C

Another experiment from Princeton University provides data that also corroborates this phenomenon. Ranney[25] followed the same experimental techniques used by Majzstrik[20] to study viscoelastic behavior of Nafion with methanol. And she also observed a transition in the Nafion membrane at zero solvent activity. Her data is shown in Figure 4-8 below.

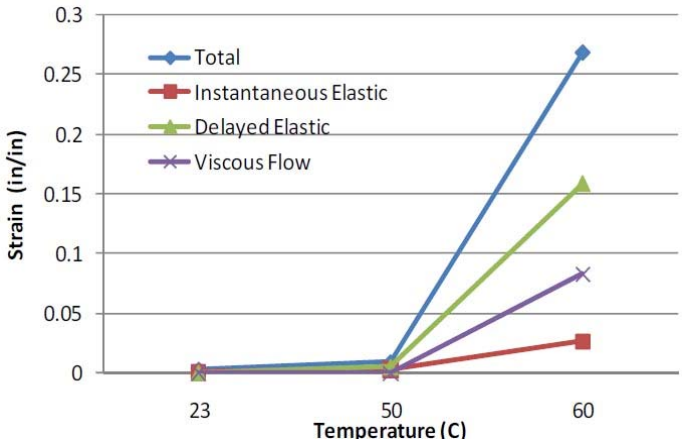

Figure 4-8 Strain vs Temperature plot, reported by [25]. Plot shows a transition region between 50°C and 60°C.

Ranney[25] also measured strain on Nafion membrane at varying temperatures and observed a transition between 50°C and 60°C.

The methanol and water sorption experiments presented in this thesis, as well as Eisenberg's[8], Majsztrik's[20], and Ranney's[25] theory and experiments of this thesis were conducted independently, yet they yielded the same conclusion on transition of Nafion membranes. Eisenberg's theory on the transition of Nafion being stabilized by electrostatic and elastic energy explains the transition that occurs in the sorption experiments, and Majsztrik's[20] and Ranney's[25] creep strain experiments, along with the experimental results of this thesis corroborate them.

One could note, however, that the transition is not so clear in methanol's sorption data. This phenomenon can again be explained by methanol's interaction with the TFE backbone. As shown in Figure 4-5, the TFE backbone is not a large barrier for methanol. Although the TFE region repels methanol's hydroxide portion, it interacts favorably with the methyl groups. This indicates that methanol's absorption will not be affected by the structural transition in Nafion. Whether clustered or randomly dispersed, the arrangement of polymer chains in Nafion will not affect absorption of methanol as it affects water

absorption; this conclusion is supported by the plot of methanol equilibrium time versus temperature.

4.2 Modeling Methanol Sorption by Nafion

4.2.1 Desorption

In the Nafion/methanol system, methanol mass uptake proceeds through convective mass transfer as methanol flowing past the Nafion membrane is picked up by the polymer surface. This phenomenon can be expressed with the equation,

$$N_A = -k_{int}(C - C_{ext}), t > 0, x = 0, l$$

N_A refers to the flux of methanol, k_{int} is the interfacial mass transfer coefficient, C is the concentration inside the membrane, and C_{ext} is the concentration in the external fluid phase (also referred to as C_∞).

For this type of behavior, the ratio between diffusive mass transfer resistance and the convective mass-transfer resistance of the fluid should be considered. This ratio is referred to as the Biot number.

$$Bi = \frac{k_{int}L}{D} \qquad \text{(Eq. 6)}$$

k_{int} L describes the external mass transfer rate while D represents the internal diffusion. When Bi<1, characteristic time of external mass transfer is greater than that of diffusion, meaning that the interfacial mass transfer is the rate-controlling mechanism.

At equilibrium, the concentration of methanol inside the membrane will reach equilibrium,

$$C = C_\infty, t \to \infty$$

Assuming that the influence of interfacial mass transport is much greater than diffusion (Bi<<1), the desorption curve can be represented by,

$$\frac{M_0 - M_t}{M_0 - M_\infty} = 1 - \exp\left[-\frac{k_{int}t}{l}\right] \qquad \text{(Eq. 7)}$$

The left side of the Eq. 7, t, and *l* are experimentally determined, and, therefore, k_{int} can be extracted for methanol, and these values are plotted for each thickness in figure 4-9.

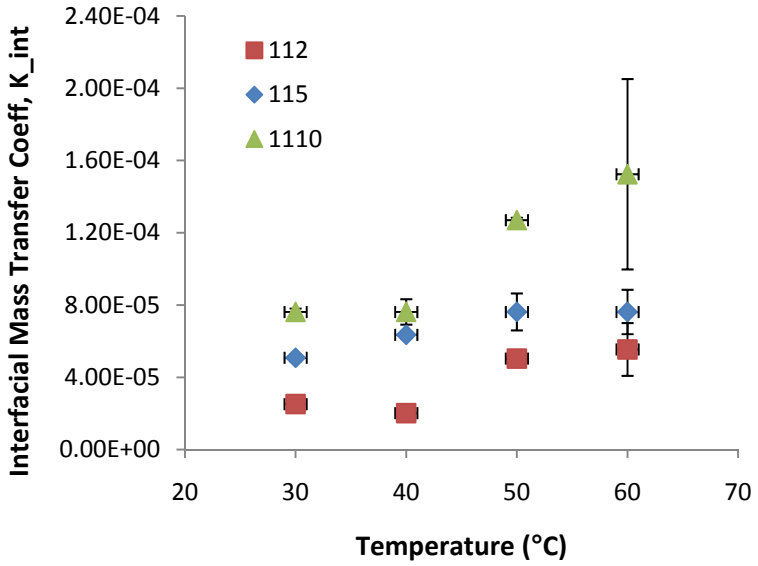

Figure 4-9 Interfacial Mass Transfer Coefficient k_{int} plotted against temperature for methanol.

The plot of $k_{int,}$ versus temperature in Figure 4-9 shows that the interfacial mass transfer coefficients for methanol at varying thicknesses and temperatures range from 2.02×10^{-5} to 1.52×10^{-4}. These values are similar to that of water, which ranges from 5×10^{-5} to 5×10^{-4}, as reported by Satterfield[28].

The mass transfer coefficients follow Arrehenius behavior, allowing us to extract activation energy values from the ln(k_{int}) versus inverse temperature plot. Activation energy values for methanol are presented in Figure 4-10 below, and are of the same order of magnitude as those for water sorption; methanol's activation energy ranges from 11.9 to 27.3 kJ/mol while that of water ranges from 22.2 to 30.6 kJ/mol, as listed in Table 4-3. These similarities in the values of interfacial mass transfer coefficient suggest that the

kinetics of methanol and water from the bulk phase to Nafion membrane does not differ significantly.

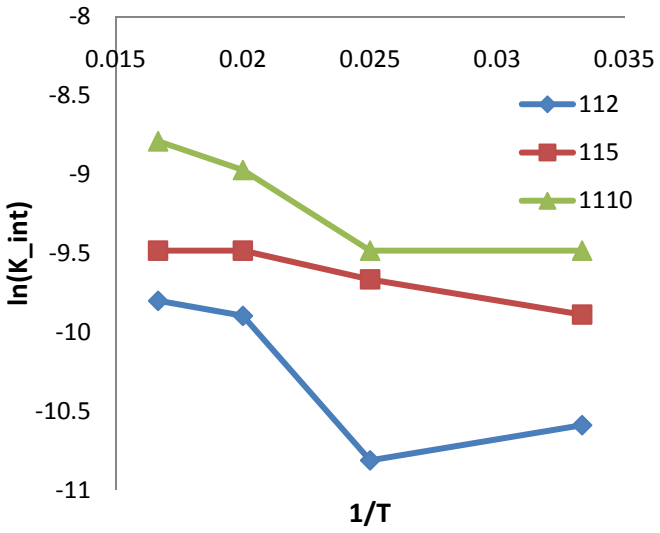

Figure 4-10 ln(k_{int}) plotted against 1/T, which yields various kinetic parameters of methanol.

Membrane Thickness (μm)	Methanol		Water[28]	
	$K_{int,0}$ (cm/s)	E_a (kJ/mol)	$K_{int,0}$ (cm/s)	E_a (kJ/mol)
112 (50.4)	1.08	27.3	0.35	22.2
115 (127)	0.00583	11.9	10.2	30.6
1110(254)	0.370	21.6	10.6	29.8

Table 4-3 Mass transfer coefficient and activation energy of methanol and water

Because absorption kinetics of methanol and water differ, these similarities in kinetic parameters might seem contradictory. However, one should keep in mind that these similarities reflect the comparable values in desorption equilibrium time. Both methanol and water desorption equilibrated around 500 seconds. In other words, while having very different absorption kinetics, water and methanol desorption are much more similar. This difference in absorption and desorption comparisons can be attributed to the reconfiguration of the polymer chains after their exposure to fluid—gas or liquid—as proposed by Goswami et al.[10] When Nafion is first exposed to the water vapor, its polymer chains reconfigure so that Nafion's hydrophilic portion will be in contact with the vapor. However, this reconfiguration is relatively unnecessary for methanol

absorption as TFE backbones can interact with methanol vapors. Goswami et al.'s [10]experimental results illustrated this difference in methanol's interaction with the TFE backbone.

4.2.2 Absorption

Satterfield[28] proposed a model for water uptake by Nafion. Her proposed model is Equation 8 below.

$$\frac{M_t - M_0}{M_\infty - M_0} = \varphi\left\{1 - exp\left[-\frac{k_{int}t}{l}\right]\right\} + (1-\varphi)\{1 - exp[-\beta t]\} \quad \text{(Eq. 8)}$$

The left side of the equation describes the proportion of mass that is picked up by the membrane. On the right side, φ represents the quasi-equilibrium constant. The quasi-equilibrium point is where the water absorption by the membrane stops responding elastically and instead is controlled by the relaxation constant. As seen from Equation 8 above, the model depends on three parameters: mass transfer coefficient $k_{int,}$ the polymer relaxation rate β, and the quasi-equilibrium constant, φ. To test Satterfield's[28] model with the methanol sorption behavior, these three parameters need to be obtained. From the analysis of methanol desorption in the previous section, k_{int} values have been obtained. Satterfield[28] reports both β values of Nafion and a φ value of 0.35 for water absorption.

For methanol, the value of φ will be different because methanol absorption did not exhibit the second phase of absorption, which is a salient feature of the water absorption curve. Thus methanol will have an φ value of 1 or very close to 1, which means that the absorption kinetics is not at all or very little dependent on the stress relaxation rate, β, of the membrane. The models have been fitted to the experimental data of methanol absorption, and two representative plots of the models are presented in Figure 4-11

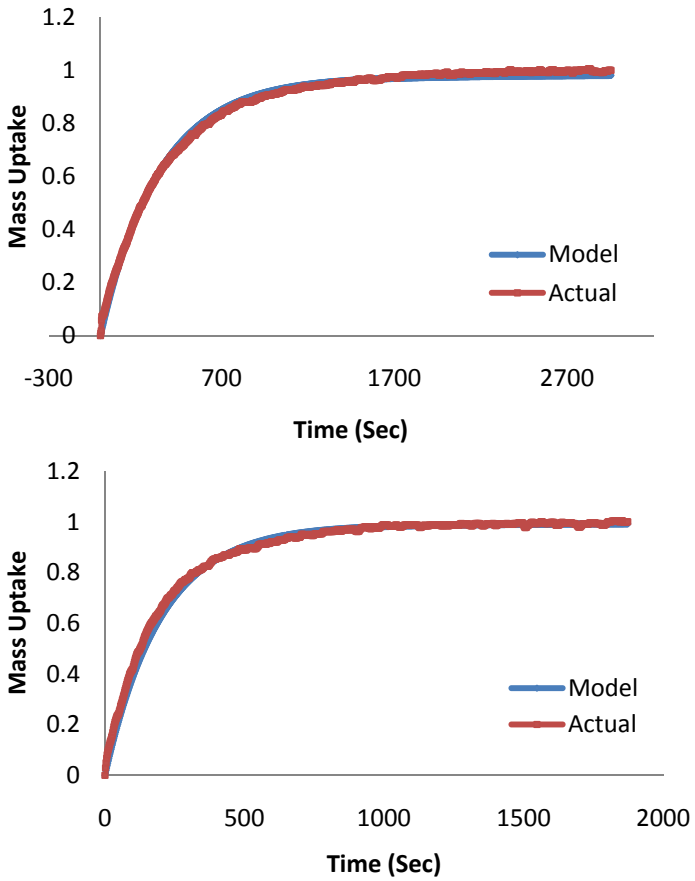

Figure 4-11 Model for methanol absorption plotted with actual data. Nafion 1110 @ 30°C (Top), Nafion 1110@50°C (Bottom)

As expected, φ values found from the models were close to 1. φ value for the 30°C model was 0.966, while that for the 50°C model was 0.980.

5. Conclusion

Sorption dynamics of methanol by Nafion was studied. PEM DMFC is the type of fuel cell system was investigated in this thesis. Methanol use in PEM DMFC has great potentials to replace petroleum-need in the transportation sector, and motivates researchers conduct careful studies on various aspects of the PEM DMFC. This thesis aimed to provide a better understanding of the PEM DMFC by scrutinizing the methanol sorption phenomenon by Nafion.

Methanol sorption by Nafion, like that of water, showed acute deviations from the Fickian diffusive model. These deviations were from conditions that were different from the ones assumed in the Fick's idealized case, such as diffusion coefficient's independence of concentration.

Results of this thesis were compared with Satterfield's[28] study of water sorption dynamics of water by Nafion. Because the experimental techniques and environment of the two researches were similar, with only the type of solvent replaced, the comparison between the two works highlighted the key differences between methanol and water as fuel for PEMFC's. First of all, the much faster absorption time for methanol led to the conclusion that methanol's structure increases the absorption speed by ~10x. The behaviors of the two absorption curves were similar, but speeds of the two had a large difference. Secondly, the two-stage sorption model, proposed by Satterfield, does not apply to the methanol sorption. Methanol's sorption behavior did not show a prominent transition throughout the experiment, which led to the conclusion that polymer relaxation rate does not play a significant role in methanol sorption phenomena. This meant that methanol's van der Waal's interaction with the TFE backbone lowered the kinetic barrier imposed by the strains on the polymer chains. This finding was made clear by the calculation of the φ value, which indicates balance between the elastic response by the Nafion membrane and the relaxation rate. When the φ value is 0, elastic response is the only entity that controls the rate, while value of 1 means that the relaxation rate is the only entity that controls the rate. Water absorption yielded a φ value of 0.35 while methanol absorption yielded values above 0.9, indicating a much smaller role of polymer relaxation in methanol sorption kinetics.

References

1. American Methanol Institue. *Beyond the Internal Combustion Engine*. Breakthrough Technologies Institute. Washington D.C.
2. Burnett, D. J.; Garcia, A. R.; Thielmann, F., Measuring Moisture Sorption and Diffusion Kinetics on Proton Exchange Membranes Using a Gravimetric Vapor Sorption Apparatus. *Journal of Power Sources* **2006,** 160, (1), 426-430.
3. Crank, J. A theoretical investigation of the influence of molecular relaxation and internal stress on diffusion in polymers. *Journal of Polymer Science* **1953,** 11, (2), 151-168.
4. Crank, J.; Henry, M. E. Diffusion in media with variable properties.1. The effect of a variable diffusion coefficient on the rates of absorption and desorption. *Transactions of the Faraday Society* **1949,** 45, (7), 636-650.
5. Crank, J.; Park, G. S. Diffusion in high polymers - Some anomalies and their significance. *Transactions of the Faraday Society* **1951,** 47, (10), 1072-1084.
6. Choi, P.; Jalani, N. H.; Datta, R. Thermodynamics and proton transport in Nafion - I. Membrane swelling, sorption, and ion-exchange equilibrium. *J Electrochem Soc* **2005**, (152), E84–E89.
7. EG&G Services, *Fuel Cell Handbook*, 5th Edition. Parsons Inc. October 2000.
8. Eisenberg, A.; Kim, J.-S. In *Introduction to Ionomers*; John Wiley & Sons, Inc.: New York, 1998, pp 164–189.
9. Ge, S. H.; Li, X. G.; Yi, B. L.; Hsing, I. M., Absorption, Desorption, and Transport of Water in Polymer Electrolyte Membranes for fuel cells. *Journal of the Electrochemical Society* **2005,** 152, (6), A1149-A1157.
10. Goswami, S.; Klaus, S.; Benziger, J. Wetting and Absorption of Water Drops on Nafion Films. *Langmuir* **2008**, (24), 8627-8633.
11. Gierke, T. D.; Munn, G. E.; Wilson, F. C., The Morphology in Nafion Perfluorinated Membrane Products, as Determined by Wide-Angle and Small-Angle X-Ray Studies.*Journal of Polymer Science Part B-Polymer Physics* **1981**, *19*, (11), 1687-1704.
12. Haubold, H.-G.; Vad, T.; Jungbluth, H.; Hiller, P. Nano structure of NAFION: a SAXS study. *Electrochim. Acta* **2001**, (*46)*, 1559.
13. Heinzel, A.; Barragán, V.M. A Review of the State-of-the-art of the Methanol Crossover in Direct Methanol Fuel Cells. *Journal of Power Sources* **1999**, *84*, (1), 70-74.
14. Hodge, I. M.; Eisenberg, A. Dielectric and Mechanical Relaxations in a Nafion Precursor. *Macromolecules* **1978**, (11), 289–293.
15. Huang, X. Y.; Solasi, R.; Zou, Y.; Feshler, M.; Reifsnider, K.; Condit, D.; Burlatsky, S.; Madden, T., Mechanical Endurance of Polymer Electrolyte Membrane and PEM Fuel Cell Durability. *Journal of Polymer Science Part B-Polymer Physics* **2006,** 44, (16), 2346-2357.
16. Jalani, N. H.; Mizar, S. P.; Choi, P.; Furlong, C.; Datta, R. Optomechanical characterization of proton-exchange membrane fuel cells. *Proc SPIE* **2004**, (5532), 316–325.
17. Kim, Y. M.; Choi, S. H.; Lee, H. C.; Hong, M. Z.; Kim, K.; Lee, H. I. Organic–inorganic composite membranes as addition of SiO_2 for high temperature-

operation in polymer electrolyte membrane fuel cells (PEMFCs). *Electrochimica Acta* **2004**, (49), 4787–4796.
18. Kyu, T.; Eisenberg, A. Mechanical Relaxations in Perfluorosulfonate Ionomer Membranes. *ACS Sympos Ser* **1982**, (180), 79–110.
19. Larmine, J.; Dicks, *A. Fuel Cell System Explained*, 2nd Edition. John Wiley&Sons: West Sussex, U.K., 2003;
20. Majsztrik, P.W. Mechanical and Transport Properties of Nafion® For PEM Fuel Cells; Temperature and Hydration Effects. Ph.D. Princeton University, 2008.
21. Mauritz, K.A.; Moore, R.B.; State of understanding of Nafion. *Chemical Review* **2004**, *104*, (10), 4535-4585.
22. Morris, D. R.; Sun, X., Water-sorption and transport properties of Nafion 117 H. *Journal of Applied Polymer Science* **1993,** 50, (8), 1445-1452.
23. Osborn, S. J.; Hassan, M. K.; Divoux, G. M.; Rhoades, D. W.; Mauritz, K. A.; Moore, R. B. Glass Transition Temperature of Perfluorosulfonic Acid Ionomers. *Macromolecules* **2007**, (40), 3886–3890.
24. Page, K. A.; Landis, F. A.; Phillips, A. K.; Moore, R. B. SAXS Analysis of the Thermal Relaxation of Anisotropic Morphologies in Oriented Nafion Membranes. *Macromolecules* **2006**, (39), 3939–3946.
25. Ranney, C. Effects of Temperature and Solvent Activity on the Viscoelastic Response of Nafion ® for PEM Fuel Cells. B.S. Princeton University, 2007.
26. Rivin, D; Kendrick, C. E.; Gibson, P. W.; Schneider, N. S. Solubility and Transport Behavior of Water and Alcohols in Nafion™ . *Polymer* **2001**, (42), (2), 623-635.
27. Satterfield, M.B.; Benziger, J.B. Viscoelastic Properties of Nafion at Elevated Temperature and Humidity. *Journal of Polymer Science Part B: Polymer Physics* **2008**, (47), (1), 11-24.
28. Satterfield, M.B.; Mechanical and Water Sorption Properties of Nafion And Composite Nafion/Titanium Dioxide Membranes For Polymer Electrolyte Membrane Fuel Cells. Ph.D. Princeton University, 2007.
29. Scott, K; Taama, W. M.; Argyropoulos, P.; Sundmacher, K.The Impact of Mass Transport and Methanol Crossover on the Direct Methanol Fuel Cell. *Journal of Power Sources* **1999**, (83), (1-2), 204-216.
30. Takamatsu, T.; Hashiyama, M.; Eisenberg, A., Sorption Phenomena in Nafion Membranes. *Journal of Applied Polymer Science* **1979,** 24, (11), 2199-2220.
31. Yang, C.; Srinivasan, S.; Bocarsly, A.B.; Tulyani, S.; Benziger, J.B. A Comparison of Physical Properties and Fuel Cell Performance of Nafion and Zirconium Phosphate/Nafion Composite Membranes. *Journal of Membrane Science* **2004**, *237*, 145-161.
32. Yang, J.H.; Bae, Y.C. Methanol Crossover Effect for Direct Methanol Fuel Cells: Applicability of Methanol Activity in Polymer Electrolyte Membrane. *J. Electrochem. Soc.* **2008**, (155), (2), B194-B199.
33. Yeo, S. C.; Eisenberg, A. Physical properties and supermolecular structure of perfluorinated ion-containing (nafion) polymers. *J Appl Polym Sci* **1977**, (21), 875–898.